

New Interpretation on the Solar Neutrino Flux with Flavor Mixing and Majorana Magnetic Moment

S. K. Kang^{a*} and C. S. Kim^{b †}

^a*School of Physics, Seoul National University, Seoul 151-734, Korea*

^b*Department of Physics, Yonsei University, Seoul 120-749, Korea*

(December 8, 2018)

Abstract

A simple and model-independent method is proposed to extract information on ν_e transition into antineutrinos via the spin flavor precession (SFP) from the measurements of solar neutrino flux at SNO and Super-Kamiokande. Incorporating the KamLAND experimental results, we examine how large the suppression of the solar neutrino flux could be due to the SFP mechanism in the context of the hybrid scenario with two-flavor neutrino and antineutrino mixings.

PACS numbers: 14.60.Pq, 14.60.St, 13.40.Em

Typeset using REVTeX

*E-mail : skkang@phya.snu.ac.kr

†E-mail : cskim@yonsei.ac.kr

Thanks to the recent neutrino experiments at Sudbury Neutrino Observatory (SNO) [1,2] and KamLAND [3], the resolution of the long-standing solar neutrino problem, discrepancy between the prediction of the neutrino flux based on the standard solar model (SSM) [4] and that measured by experiments, is just around corner. In addition to the radiochemical experiments on *Ga* and *Cl* targets for solar neutrinos, the water Cerenkov experiments from Super-Kamiokande (SK) [5] has observed the emitted electron from elastic scattering (*ES*) $\nu_x + e \rightarrow \nu_x + e$, ($\nu_x = \nu_e, \nu_\mu, \nu_\tau$), while SNO has measured the neutrino flux through the charged current (*CC*) process $\nu_e + d \rightarrow p + p + e$, the neutral current (*NC*) process $\nu + d \rightarrow \nu + p + n$, and *ES* process given in the above. Both the experiments, SNO and SK, probe the high energy tail of the solar neutrino spectrum, which is dominated by the 8B neutrino flux. The results of the solar neutrino flux measured at SK and SNO are as follows [2,5]:

$$\Phi_{\text{SNO}}^{CC} = 1.76 \pm 0.11 \times 10^6 \text{cm}^{-2} \text{s}^{-1}, \quad (1)$$

$$\Phi_{\text{SNO}}^{ES} = 2.39 \pm 0.27 \times 10^6 \text{cm}^{-2} \text{s}^{-1}, \quad (2)$$

$$\Phi_{\text{SK}}^{ES} = 2.35 \pm 0.08 \times 10^6 \text{cm}^{-2} \text{s}^{-1}, \quad (3)$$

$$\Phi_{\text{SNO}}^{NC1} = 5.09 \pm 0.63 \times 10^6 \text{cm}^{-2} \text{s}^{-1}, \quad (4)$$

$$\Phi_{\text{SNO}}^{NC2} = 6.42 \pm 1.67 \times 10^6 \text{cm}^{-2} \text{s}^{-1}, \quad (5)$$

where Φ_{SNO}^{NC1} was found assuming undistorted 8B neutrino energy spectrum, while Φ_{SNO}^{NC2} was found when this assumption was relaxed. Comparing those results with the prediction of the SSM, $\Phi_{\text{SSM}} = 5.05_{-0.81}^{+1.01} \times 10^6 \text{cm}^{-2} \text{s}^{-1}$ [4], we confirm the flux deficit of solar neutrino. It is commonly believed that the most plausible solution of the solar neutrino anomaly is in terms of neutrino oscillation, and in particular the oscillation of ν_e into another active flavor ν_a , which can be any combination of ν_μ and ν_τ . Based on a global analysis in the framework of two-active neutrino oscillations of all solar neutrino data, the large mixing angle (LMA) solution is favored and oscillations into a pure sterile state are excluded at high confidence level [6]. On the other hand, the KamLAND collaboration [3] has found for the first time the evidence for the disappearance of reactor antineutrinos, which confirms LMA solution of

the solar neutrino problem for the CPT invariant neutrino mass spectrum. It appears that all non-oscillation solutions of the solar neutrino problem are strongly disfavored [7].

The spin flavor precession (SFP) solution of the solar neutrino problem [8], motivated by the possible existence of nonzero magnetic moments of neutrinos, has also been studied and found to have a good fit slightly better than the LMA oscillation solution before the KamLAND experiment. Although the KamLAND result excludes a *pure* SFP solution to the solar neutrino problem under the CPT invariance, a fraction of the flux suppression of solar neutrino may still be attributed to SFP [9,10]. In this respect, we believe that the detailed investigation on how much the flux suppression of solar neutrino can be attributed to SFP will lead us to make considerable progress in understanding the solar neutrino anomaly as well as the inner structure of the Sun. In this Letter, we propose a simple and model-independent method to extract information on ν_e transition into antineutrinos via SFP from the measurements of 8B neutrino flux at SNO and SK. As will be seen, in particular, our determination of the mixing between non-electron active neutrino and antineutrino is not affected by the existence of transition into a sterile state. In addition, we study the implication of KamLAND results on the hybrid scenario with both neutrino oscillation and SFP conversion.

Let us begin by considering how the experimental measurement of the solar neutrino flux can be presented in terms of the solar neutrino survival probability. In this study, we use *ES* measurement of SK instead of corresponding measurement of SNO, and take Φ_{SNO}^{NC1} as *NC* flux because of a smaller error. Assuming the SSM neutrino fluxes and the transition of ν_e into a mixture of active flavor ν_a and sterile ν_s , $\nu_a \sin \alpha + \nu_s \cos \alpha$, that participate in the solar neutrino oscillations, one can write the SK *ES* rate and the SNO *CC* and *NC* scattering rates relative to the SSM predictions in terms of the survival probability [11,12]:

$$R_{\text{SK}}^{ES} \equiv \Phi_{\text{SK}}^{ES}/\Phi_{\text{SSM}} = f_B[P_{ee} + r \sin^2 \alpha(1 - P_{ee})], \quad (6)$$

$$R_{\text{SNO}}^{CC} \equiv \Phi_{\text{SNO}}^{CC}/\Phi_{\text{SSM}} = f_B P_{ee}, \quad (7)$$

$$R_{\text{SNO}}^{NC} \equiv \Phi_{\text{SNO}}^{NC}/\Phi_{\text{SSM}} = f_B[P_{ee} + \sin^2 \alpha(1 - P_{ee})], \quad (8)$$

where $r = \sigma_{\nu_a}^{NC} / \sigma_{\nu_e}^{CC+NC} \simeq 0.171$ is the ratio of $\nu_{\mu,\tau}$ to ν_e *ES* cross-sections [14], and P_{ee} is the ν_e survival probability. Here $\sin^2 \alpha$ indicates the fraction of ν_e oscillation to active flavor ν_a . Since there is a large uncertainty in the predicted normalization, Φ_{SSM} , arising from the uncertainty in the ${}^7\text{Be} + p \rightarrow {}^8\text{B} + \gamma$ cross-section, we have introduced a constant parameter f_B to denote the normalization of the ${}^8\text{B}$ neutrino flux relative to the SSM prediction. It should be also noted here that the SK *ES* and SNO *CC* data start from neutrino energies of 5 and 7 MeV respectively, while the response function of the SNO *NC* measurement extends marginally below 5 MeV. However, the SK rate and the resulting survival probability show energy independence down to 5 MeV to a very good precision. The SNO *CC* rate shows energy independence as well, although to lesser precision. Therefore, it is reasonable to assume a common survival probability for all the three measurements. Using the measured values of the rates R , we can estimate the allowed regions of the quantities f_B, P_{ee} and α . In particular, the fraction of ν_e oscillation to ν_a is described by the relation,

$$\sin^2 \alpha = \frac{R_{\text{SK}}^{ES} - R_{\text{SNO}}^{CC}}{r(f_B - R_{\text{SNO}}^{CC})}. \quad (9)$$

As is well known, a family of the present solar neutrino experiments is not enough to extract the value of α because of the unknown parameter f_B . This is so-called the α, f_B degeneracy [11]. The recent analysis shows that a pure sterile oscillation solution ($\sin^2 \alpha = 0$) is disfavored and $0.14 \leq \sin^2 \alpha \leq 1$ is obtained for $f_B \leq 2$ from the χ^2 analysis at the 1σ level [11].

Model independent analysis for SFP + Oscillation :

So far, we have considered only the possible ν_e conversion to the active and sterile neutrinos. The excess *NC* and *ES* events can also be caused by the antineutrinos. The antineutrinos in question must be of the muon or tau types, since $\bar{\nu}_e$ would be easily identified through the reaction $\bar{\nu}_e + p \rightarrow n + e^+$ [13]. Both $\nu_{\mu,\tau}$ and $\bar{\nu}_{\mu,\tau}$ scatter on electrons and deuterium nuclei through their *NC* interactions, with different cross sections. The $\nu_e \rightarrow \nu_{\mu,\tau}$ conversion is predicted in the flavor oscillation scenario, while $\nu_e \rightarrow \bar{\nu}_{\mu,\tau}$ is predicted in the neutrino SFP scenario [8]. When we allow the possible conversion to the antineutrinos, the previous

formula (6) for the SK ES rate relative to the SSM prediction is modified as follows:

$$R_{\text{SK}}^{ES} = f_B(P_{ee} + r \sin^2 \alpha \sin^2 \psi (1 - P_{ee}) + \bar{r} \sin^2 \alpha \cos^2 \psi (1 - P_{ee})), \quad (10)$$

where $\bar{r} = \sigma_{\bar{\nu}_a}^{NC} / \sigma_{\nu_e}^{CC+NC} \simeq 0.114$ and ψ is a mixing angle that describes the linear combination of the probability of ν_e conversion into ν_a and active antineutrinos. Assuming the conversions between two families, we have $\tan^2 \psi = P(\nu_e \rightarrow \nu_\mu) / P(\nu_e \rightarrow \bar{\nu}_\mu)$.

From Eqs. (7,8,10), we see that the mixing angle ψ is related with the measured neutrino fluxes as follows:

$$r \sin^2 \psi + \bar{r} \cos^2 \psi = \frac{R_{\text{SK}}^{ES} - R_{\text{SNO}}^{CC}}{R_{\text{SNO}}^{NC} - R_{\text{SNO}}^{CC}}, \quad (11)$$

where we have assumed that $\sin^2 \alpha$ is non-zero. The expression (11) shows that the determination of the mixing angle ψ is independent of $\sin^2 \alpha$. While the mixing angle α could not be determined from the SNO and SK data due to the α, f_B degeneracy, it appears that we are led to determine the mixing angle ψ from those data. As one can see from Eq. (11), the precise measurements of $R_{\text{SK}}^{ES}, R_{\text{SNO}}^{NC}, R_{\text{SNO}}^{CC}$ as well as the values of r and \bar{r} make it possible to see how much the solar neutrino flux deficit can be caused by SFP. We note that any deviation of the value of $\sin^2 \psi$ from one implies the evidence for the existence of ν_e transition into non-sterile antineutrinos, and if there is no transition of solar neutrino due to the magnetic field inside the sun, the left-hand side of Eq. (11) should be identical to the parameter r . Using the experimental data, we obtain the values for the right-hand side of Eq. (11):

$$0.169 \pm 0.053. \quad (12)$$

We see that the central value is close to the value of r for the energy threshold of SNO and SK, which implies that the best fit corresponds to the very small possibility of $\nu_e \rightarrow \nu_a$ transition even if large possibility of such a transition is allowed. Since $\bar{r} \leq r \sin^2 \psi + \bar{r} \cos^2 \psi \leq r$, we notice that the left-hand side of Eq. (11) prefers to lower side of Eq. (12). The central value

of Eq. (12) leads to $\sin^2 \psi = 0.94$. Since the error in Eq. (12) which leads to $\delta \sin^2 \psi = 0.93$ is rather large, we cannot obtain any severe constraint on the mixing angle ψ from the present solar neutrino experimental results, but we can say that the spin-flavor transition due to neutrino magnetic moment is allowed in the light of the high energy solar neutrino experiments, SNO and SK. In the future, experiments may lead the error in Eq. (12) to be reduced so that a lower bound on the mixing angle ψ could be obtained. For example, if the future SNO experiments could reduce the error in charged current measurement to 50%, then the uncertainty on $\sin^2 \psi$ becomes 0.76, and if the errors in both charged and neutral current experiments could be reduced to 50%, the uncertainty on $\sin^2 \psi$ becomes 0.60. Therefore, there is room for resolving the solar neutrino flux deficit through both neutrino oscillation and SFP.

Implication of KamLAND :

The recent reactor neutrino measurement at KamLAND implies the existence of ν_e oscillation in vacuum. The allowed regions for the vacuum mixing angle and Δm^2 at 3σ are given by [7]

$$\begin{aligned} 0.29 &\leq \tan^2 \theta \leq 0.86, \\ 5.1 \times 10^{-5} \text{eV}^2 &\leq \Delta m^2 \leq 9.7 \times 10^{-5} \text{eV}^2, \\ 1.2 \times 10^{-4} \text{eV}^2 &\leq \Delta m^2 \leq 1.9 \times 10^{-4} \text{eV}^2. \end{aligned} \tag{13}$$

The local minimum occurs for $\tan^2 \theta = 0.42$, $\Delta m^2 = 1.4 \times 10^{-4} \text{eV}^2$. In the light of KamLAND experimental result, the large mixing angle MSW solution of the solar neutrino problem is strongly favored [7]. Let us consider the implication of the KamLAND result on the solar neutrino problem when we allow both neutrino oscillation and SFP mechanism as discussed in the previous section. As will be shown later, in order to determine both neutrino conversion effects, we need to know the mixing angle and Δm^2 in vacuum as well as the information on the Sun such as matter density and magnetic field profile inside the Sun. In this Letter, we will take the KamLAND results to fix the mixing angle and Δm^2 in vacuum and then investigate how the parameters concerned with the Sun can be constrained by the

SNO and SK experiments.

Assuming two Majorana families, ν_e and ν_μ , without sterile sectors, the evolution equations for the two families can be presented in terms of 4×4 Hamiltonian matrix in the basis $(\nu_e, \nu_\mu, \bar{\nu}_e, \bar{\nu}_\mu)$ in a nonzero transverse magnetic field as given in Ref. [15]

$$H = \begin{pmatrix} a_{\nu_e} & \frac{\Delta m^2}{4E_\nu} \sin 2\theta & 0 & \mu_\nu^* B \\ \frac{\Delta m^2}{4E_\nu} \sin 2\theta & \frac{\Delta m^2}{2E_\nu} \cos 2\theta + a_{\nu_\mu} & -\mu_\nu^* B & 0 \\ 0 & -\mu_\nu B & -a_{\nu_e} & \frac{\Delta m^2}{4E_\nu} \sin 2\theta \\ \mu_\nu B & 0 & \frac{\Delta m^2}{4E_\nu} \sin 2\theta & \frac{\Delta m^2}{2E_\nu} \cos 2\theta - a_{\nu_\mu} \end{pmatrix} \quad (14)$$

where μ_ν is neutrino magnetic moment and B is magnetic field strength inside the Sun and $a_{\nu_e} = G_\mu/\sqrt{2}(2N_e - N_n)$, $a_{\nu_\mu} = G_\mu/\sqrt{2}(-N_n)$ where N_e and N_n are the densities of electron and neutrons in the Sun. This Hamiltonian can be diagonalized exactly by

$$X = \begin{pmatrix} c^a & s^a & 0 & 0 \\ -s^a & c^a & 0 & 0 \\ 0 & 0 & c^b & s^b \\ 0 & 0 & -s^b & c^b \end{pmatrix} \begin{pmatrix} 1 & 0 & 0 & 0 \\ 0 & c' & s' & 0 \\ 0 & -s' & c' & 0 \\ 0 & 0 & 0 & 1 \end{pmatrix} \begin{pmatrix} c'' & 0 & 0 & s'' \\ 0 & 1 & 0 & 0 \\ 0 & 0 & 1 & 0 \\ -s'' & 0 & 0 & c'' \end{pmatrix} \quad (15)$$

where $s^a = \sin \theta^a$, $s' = \sin \theta'$ and $s'' = \sin \theta''$ and c^a, c', c'' correspond to the cosines of the mixing angles. For simplicity, let us consider the adiabatic approximation which implies slowly changing magnetic field and matter density inside the Sun. Then, without the oscillating term, transition probabilities are simply given as follows:

$$P(\nu_e \rightarrow \nu_e) = \cos^2 \theta_p'' (\cos^2 \theta \cos^2 \theta_p^a + \sin^2 \theta \sin^2 \theta_p^a), \quad (16)$$

$$P(\nu_e \rightarrow \nu_\mu) = \cos^2 \theta_p' (\cos^2 \theta \sin^2 \theta_p^a + \sin^2 \theta \cos^2 \theta_p^a), \quad (17)$$

$$P(\nu_e \rightarrow \bar{\nu}_\mu) = \sin^2 \theta_p'' (\cos^2 \theta \cos^2 \theta_p^a + \sin^2 \theta \sin^2 \theta_p^a), \quad (18)$$

$$P(\nu_e \rightarrow \bar{\nu}_e) = \sin^2 \theta_p' (\cos^2 \theta \sin^2 \theta_p^a + \sin^2 \theta \cos^2 \theta_p^a), \quad (19)$$

where θ is the mixing angle in vacuum, whereas θ_p', θ_p'' and θ_p^a are the mixing angles at the production point of ν_e inside the Sun. Note that the mixing angles θ_p' and θ_p'' depend on $\mu B, \theta, \Delta m^2/E_\nu$ as well as the matter densities a_{ν_e} and a_{ν_μ} . Non-adiabatic case as well as the

details on the mixing matrix X and the exact expressions of the probabilities will be studied elsewhere [16]. When neutrinos are produced in the region where the matter density is far above the resonance region ($a_{\nu_e} - a_{\nu_\mu} = \Delta m^2/(2E_\nu)$), θ_p^a is close to $\pi/2$ at the production point as in the case of MSW solution. We also note that there are no resonance regions for θ_p' and θ_p'' [16].

The bound on the probability $P(\nu_e \rightarrow \bar{\nu}_e) \leq 1.5\%$ [9] may lead us to see how large are the values of parameters concerned with solar magnetic field such as μB , θ_p' and θ_p'' . For given values of θ_p^a and θ , we can obtain some bound on θ_p' which in turn leads us to bounds on the parameters such as μB , θ_p'' and ψ . In particular, in the limit of $\theta_p^a = \pi/2$, we note that the relations, $(\mu B)^2 = a_{\nu_e}^2 \tan^2 2\theta_p'$, holds and the mixing angle ψ can be presented in terms of θ , θ_p' , and θ_p'' , $\sin^2 \psi \simeq 1 - \sin^2 \theta_p'' / \tan^2 \theta \cos^2 \theta_p'$. In our numerical analysis, we consider several cases with fixed values of $\sin^2 \theta_p'$ which correspond to the current bound and soon achievable sensitivities on $P(\nu_e \rightarrow \bar{\nu}_e)$. Imposing the KamLAND results given in Eq.(13) and $\theta_p^a \sim \pi/2$, we can estimate the allowed regions of the parameters θ_p'' and ψ . This procedure makes us to predict the possible values of the survival probability $P(\nu_e \rightarrow \nu_e)$. We have also found that the numerical results are not sensitive to 8B neutrino energies E_ν measured in SK and SNO. In Fig. 1, we plot $P(\nu_e \rightarrow \nu_e)$ vs. μB for $P_{e\bar{e}} =$ (a) 0.015, (b) 0.005, (c) 0.001 and (d) 0.0001. The solid lines show how the value of $P(\nu_e \rightarrow \nu_e)$ depends on μB for the allowed ranges of θ , $\Delta m^2/E_\nu$ and fixed values of $P_{e\bar{e}}$. The two vertical lines in Fig. 1 are the upper and lower limits on the allowed region of $P(\nu_e \rightarrow \nu_e)$ at 1σ from the solar neutrino experimental results, $P(\nu_e \rightarrow \nu_e) = 0.35 \pm 0.07$ assuming $f_B = 1$ [11,12]. In Fig. 2, we plot $P(\nu_e \rightarrow \nu_e)$ vs. $\sin^2 \psi$ for the same fixed values of $P(\nu_e \rightarrow \bar{\nu}_e)$ as in Fig. 1. The two vertical lines are also the same as in Fig. 1. Here, we note that any deviation of $\sin^2 \psi$ from one implies the existence of solar ν_e transition into active antineutrinos via SFP mechanism. As one can see from Fig. 2, there is some region of $\sin^2 \psi$ deviated from one which is consistent with the current solar neutrino observations and KamLAND experiment. We can obtain a bound on $\sin^2 \psi \sim 0.76$ which corresponds to $P(\nu_e \rightarrow \nu_e) \sim 0.28$ and the case of $P(\nu_e \rightarrow \bar{\nu}_e) = 0.015$. As anticipated, $\sin^2 \psi$ approaches to one as $P(\nu_e \rightarrow \bar{\nu}_e)$ becomes

smaller. From the results, we see that some part of the suppression of solar neutrino flux may be due to the conversion of ν_e to $\bar{\nu}_\mu$ via SFP mechanism although it is not without any uncertainty. Thus, we conclude that the hybrid scenario with both neutrino oscillation and SFP conversion may be presently consistent with solar neutrino experiments and KamLAND result.

In summary, we have proposed a simple and model-independent method to extract information on ν_e transition into antineutrinos via SFP from the measurements of solar neutrino flux at SNO and SK. But, from the current solar neutrino experiments, we could not obtain any severe constraint as to how large ν_e transition into antineutrinos via SFP could be. Incorporating the KamLAND experimental results, we have examined how large the suppression of solar neutrino flux could be due to the SFP mechanism in the context of the hybrid scenario with two-flavor neutrino and antineutrino mixings.

S.K.K is supported by and by BK21 program of the Ministry of Education in Korea, and by Korea Research Foundation Grant (KRF-2002-015-CP0060). The work of C.S.K. was supported by Grant No. R02-2003-000-10050-0 from BRP of the KOSEF.

REFERENCES

- [1] Q. R. Ahmad *et al.* [SNO Collab.], Phys. Rev. Lett. **87**, 071301 (2001).
- [2] Q. R. Ahmad *et al.* [SNO Collab.], Phys. Rev. Lett. **89**, 011301 (2002).
- [3] K. Eguchi *et al.* [KamLAND Collab.], Phys. Rev. Lett. **90**, 021802 (2003).
- [4] J. N. Bahcall, M. C. Gonzalez-Garcia and C. Pena-Garay, Circrophys. J. **555**, 990 (2001).
- [5] S. Hukuda *et al.* [Super-Kamiokande Collab.], Phys. Rev. Lett. **86**, 5656 (2001); S. Hukuda *et al.* [Super-Kamiokande Collab.], Phys. Lett. **539**, 179 (2002).
- [6] V. Barger, D. Marfatia, K. Whisnant and B. P. Wood, Phys. Lett. **B537**, 179 (2002).
- [7] M. Maltoni, T. Schwetz and J. W. F. Valle, arXiv:hep-ph/0212129; G.L. Fogli, E. Lisi, A. Palazzo and A. M. Rotunno, arXiv:hep-ph/0211414.
- [8] See for example, E. Akhmedov, arXiv:hep-ph/9705451; E. Akhmedov and Joao Pulido, Phys. Lett.**B 485**, 178 (2000).
- [9] E. Kh. Akhmedov and J. Pulido, Phys. Lett. **553**, 7 (2003).
- [10] D. O. Caldwell and P. A. Sturrock, hep-ph/0305303.
- [11] V. Barger, D. Marfatia and K. Whisnant, Phys. Rev. Lett. **88**, 011302 (2002).
- [12] A. Aguilar-Arevalo and J. Dolivo, Phys. Rev. **D66**, 113009 (2002); A. Bandyopadhyay *et al.*, Phys. Lett. **B540**, 14 (2002); P.C. de Holanda and A. Yu. Smirnov, hep-ph/0211264.
- [13] P. Vogel and J. F. Beacom, Phys. Rev. **D 60**, 053003 (1999).
- [14] J. N. Bahcall, M. Kamionkowski and A. Sirlin, Phys. Rev. **D51**, 6146 (1995).
- [15] W. Marciano and C. S. Lim, Phys. Rev. **D 37**, 1368 (1988).
- [16] S. K. Kang and C. S. Kim, work in progress.

FIGURES

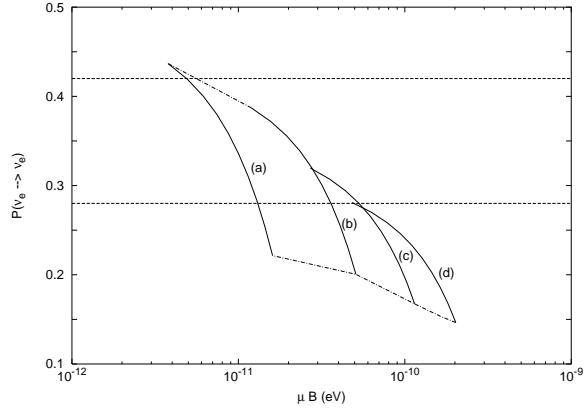


FIG. 1. The prediction of $P(\nu_e \rightarrow \nu_e)$ as a function of μB for the ranges of $\tan^2 \theta$ and Δm^2 given in Eq. (13) and $P(\nu_e \rightarrow \bar{\nu}_e) =$ (a) 0.015, (b) 0.005, (c) 0.001 and (d) 0.0001. The two vertical lines correspond to the upper and lower limits on $P(\nu_e \rightarrow \nu_e)$ at 1σ from the solar neutrino experimental results.

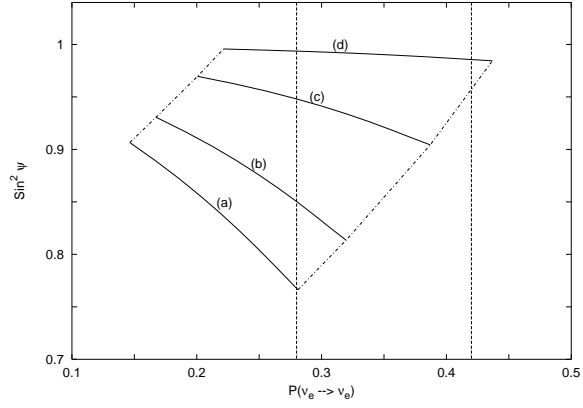


FIG. 2. Plot of $P(\nu_e \rightarrow \nu_e)$ vs. $\sin^2 \psi$ for the ranges of $\tan^2 \theta$ and Δm^2 given in Eq. (13) and the same fixed values of $P(\nu_e \rightarrow \bar{\nu}_e)$ as in Fig. 1. The two vertical lines are also the same as in Fig. 1.